

PAPER • OPEN ACCESS

Inducing upwards band bending by surface stripping ZnO nanowires with argon bombardment

To cite this article: Chris J Barnett *et al* 2020 *Nanotechnology* **31** 505705

View the [article online](#) for updates and enhancements.




IOP | ebooks™

Bringing together innovative digital publishing with leading authors from the global scientific community.

Start exploring the collection—download the first chapter of every title for free.

Inducing upwards band bending by surface stripping ZnO nanowires with argon bombardment

Chris J Barnett^{1,5} , Jorge Navarro-Torres², James D McGettrick², Thierry G G Maffei² and Andrew R Barron^{1,3,4}

¹ Energy Safety Research Institute, Swansea University, Bay Campus, Swansea SA1 8EN, United Kingdom

² College of Engineering, Swansea University, Bay Campus, Swansea SA1 8EN, United Kingdom

³ Department of Chemistry and Department of Materials Science and Nanoengineering, Rice University, Houston, Texas 77005, United States of America

⁴ Faculty of Engineering, Universiti Teknologi Brunei, Jalan Tungku Link, Gadong BE1410, Brunei

E-mail: c.j.barnett@swansea.ac.uk

Received 18 May 2020, revised 17 August 2020

Accepted for publication 28 August 2020

Published 2 October 2020



CrossMark

Abstract

Metal oxide semiconductors such as ZnO have attracted much scientific attention due their material and electrical properties and their ability to form nanostructures that can be used in numerous devices. However, ZnO is naturally n-type and tailoring its electrical properties towards intrinsic or p-type in order to optimise device operation have proved difficult. Here, we present an x-ray photon-electron spectroscopy and photoluminescence study of ZnO nanowires that have been treated with different argon bombardment treatments including with monoatomic beams and cluster beams of 500 atoms and 2000 atoms with acceleration volte of 0.5 keV–20 keV. We observed that argon bombardment can remove surface contamination which will improve contact resistance and consistency. We also observed that using higher intensity argon bombardment stripped the surface for nanowires causing a reduction in defects and surface OH⁻ groups both of which are possible causes of the n-type nature and observed a shift in the valance band edge suggest a shift to a more p-type nature. These results indicate a simple method for tailoring the electrical characteristic of ZnO.

Supplementary material for this article is available [online](#)

Keywords: ZnO, nanowires, argon bombardment, XPS, ohmic, Schottky, photoluminescence,

(Some figures may appear in colour only in the online journal)

1. Introduction

ZnO is a metal-oxide semiconductor with a wide band gap of 3.37 eV and properties that include high transparency, a large

piezoelectric constant, room temperature ferromagnetism, thermal and mechanical stability and the ability to form numerous nanostructures [1, 2]. These properties have led to ZnO nanostructures being used in a number of devices including field effect transistors, gas, chemical and bio sensors, LEDs, and solar cells. [2–4] In order for these devices to operate efficiently the electrical properties of the ZnO must be optimised. However, ZnO is naturally n-type which makes it difficult to dope into p-type or even an intrinsic state, therefore limiting the efficiency of devices and the potential applications of ZnO.

⁵ Author to whom any correspondence should be addressed



Original content from this work may be used under the terms of the [Creative Commons Attribution 4.0 licence](#). Any further distribution of this work must maintain attribution to the author(s) and the title of the work, journal citation and DOI.

A number of groups have carried out surface modifications to ZnO nanowires including Liu *et al* who observed that covering ZnO nanowires with PMMA reduced defects at the surface that caused surface charge and n-type behaviour [5]. While a study published by Richters *et al* observed similar effects by in casing ZnO nanowires in Al₂O₃ [6]. Recent work by Dastjerdi *et al* used hydrogen plasma to passivate surface states of ZnO nanowires and caused a reduction in defects observed with photoluminescence (PL) [7]. Other work carried out by Allen *et al* has shown that reactive oxygen species at the surface can influence the electrical properties and contact type [8, 9]. Their work has also shown it is possible to alter the surface band bending by depositing aryldiazonium salt using electrochemistry and annealing and therefore shifting ZnO towards a more intrinsic behaviour [10].

In our previous work we used argon bombardment to strip the surface of ZnO nanorods and nanosheets and observed a shift from near ohmic to rectifying contacts when carrying out nanoscale 2 point probe suggesting a shift from n-type towards p-type [11, 12]. We also observed a reduction in the deep level emission (DLE) peak of the PL spectra suggesting the defects are related to the n-type nature of ZnO and that they are situated at the near surface. Recent work by Kennedy *et al* involving electron microscopy—cathodoluminescence has also suggested that defects such as oxygen vacancies are situated at the near surface of ZnO nanowires [13].

Here we have carried out XPS on an array of ZnO nanowires and carried out argon bombardment *in situ* to measure chemical changes and to measure any shift in the valence band to confirm our previous works assumption that removing defects by surface stripping can shift ZnO nanowires from n-type towards intrinsic.

2. Method

ZnO nanowires arrays were synthesised on Si wafers with a native oxide that had been cleaned using sonication in acetone and isopropanol. The ZnO seed layer was deposited by spin coating a 54 mM solution of zinc acetate, seven layers were deposited and after each coating the sample was annealed at 60 °C for 5 min and finally the substrate was annealed at 360 °C to ensure all the acetate has converted to zinc oxide. For the nanowire growth, the coated substrate was floated seed layer down in a 500 ml solution containing 3.62 g zinc nitrate and 1.50 g hexamine at 90 °C for 6 h [14]. The sample was then rinsed in DI water and allowed to dry in air. The sample was then scored using a diamond scribe into seven 3 × 3 mm areas.

The sample was loaded in a Kratos Axis Supra XPS equipped with a Minibeam 6 gas Cluster Ion Source, base pressure $\sim 10^{-9}$ mbar. XPS spectra were collected on each of the seven marked areas before and after argon bombardment with each area subjected to a different treatment in terms of dose, power and type (cluster versus monoatomic beams). One area was not treated with argon to act as a control, one area was treated with a 2000 atom cluster beam accelerated at 5 keV (here after referred to as 5 keV Ar⁺₂₀₀₀), three areas

where treated with a 500 atom cluster beam with accelerations of 5 keV (here after referred to as 5 keV Ar⁺₅₀₀), 10 keV (here after referred to as 10 keV Ar⁺₅₀₀) and 20 keV (here after referred to as 20 keV Ar⁺₅₀₀), and the final two areas where treated with a monoatomic beam with accelerations of 0.5 keV and 5 keV (here after referred to as 0.5 keV Ar⁺_{Mono} and 5 keV Ar⁺_{Mono}, respectively). The order listed here ranges from least to most aggressive in terms of etching power, with larger cluster being less aggressive due to energy being distributed to each atom in the cluster, i.e. each argon atom in a 500 cluster at 20 keV would have an energy of 0.04 keV [15].

After argon treatment each area of the sample was characterised using a Hitachi S4800 SEM and PL using a 325-nm wavelength He-Cd laser and an Ocean Optics USB2000+ spectrometer.

3. Results and discussion

SEM images (figure 1) of the as grow nanowires show that they are of hexagonal form with a wide range of diameters. Measurement across the top facet using the SEM's inbuilt measuring tools from multiple areas across the sample indicated the nanowires diameters generally ranged from 40 nm to 300 nm, although some may be significantly smaller than this. The SEM images show that there is no apparent change to the nanowire surfaces in the areas that have been subjected to cluster argon bombardment. Figure 2(b) does show some darkening on one nanowire which could indicate potential damage, however, we can find no other damage in the SEM images from this treatment and therefore attribute it to a growth defect or electron shadowing. In contrast, both areas treated with the monoatomic beam show potential damage indicating that the surface has been stripped by the bombardment. These areas are indicated by green squares.

Argon bombardment is often used to remove surface contamination [16] and in our previous work we suggested that the surface stripping of ZnO nanostructures by argon bombardment changed the electronic structure by reducing the n-type donors and we observed a shift from ohmic to Schottky contacts. X-ray photon-electron spectroscopy (XPS) can show chemical and electronic changes in samples and has been used here to characterise the ZnO nanowires before and after each treatment. Here XPS scans have been recorded before and after each argon treatment including a survey scan, figure 2(a)), and detailed scans of the Zn 2p, O 1s, Ar 2p, C 1s, Si 2p, Zn LMM at ~ 990 eV KE, and the valence band edge. The survey scans show no observable deviation all chemical elements remain after Ar bombardment and the composition is shown in table S1 (<https://stacks.iop.org/NANO/31/505705/mmedia>) in the supplemental information. Si 2p was scanned to ensure there was no contribution from the native oxide of the silicon substrate. The XPS scans are shown in the supplemental information and show that no silicon was present. The scans for Ar 2p (supplemental information, figure S1) also did not show the presence of argon after bombardment indicating that the argon had not been incorporated into the structure. The Zn (LMM) scan

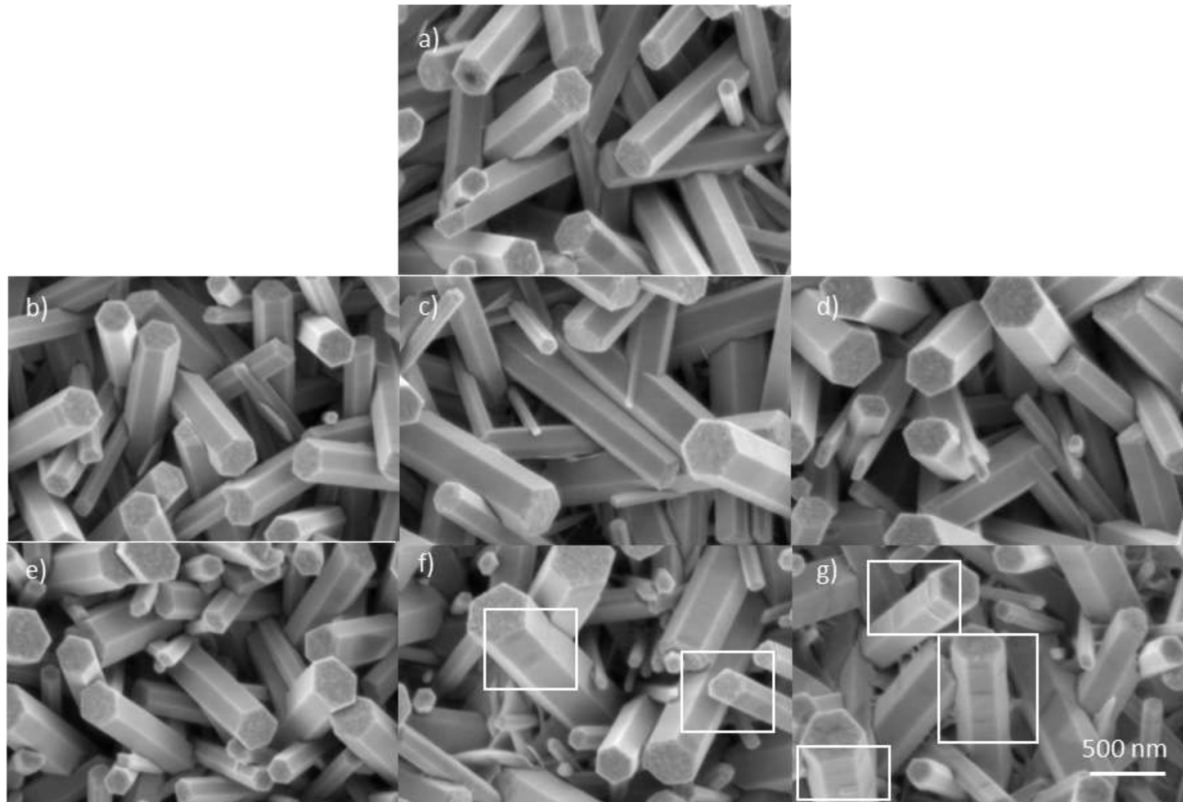


Figure 1. SEM images of ZnO nanowires (a) as grown and after argon bombardment at (b) 5 keV Ar^+_{2000} , (c) 5 keV Ar^+_{500} , (d) 10 keV Ar^+_{500} , (e) 20 keV Ar^+_{500} , (f) 0.5 keV $\text{Ar}^+_{\text{Mono}}$ and (g) 5 keV $\text{Ar}^+_{\text{Mono}}$. White squares highlight potential areas of damage.

(supplemental information, figure S1) shows argon treatment did not alter significantly alter the nanorods from ZnO to Zn metal.

In our previous work we attribute the improvement in contact consistency to the removal of adventitious carbon by argon bombardment. [11, 12] table 1 shows that the carbon percentage before argon treatment ranged from 16% to 29%, depending on the location on the substrate. The shape and position of the C 1s peak did not shift after argon bombardment, however, from table 1 the quantity of carbon reduced in line with the dose. The 5 keV $\text{Ar}^+_{\text{Mono}}$ treatment, show in figure 2(b) reduced the carbon from 17% to 4% while the 5 keV Ar^+_{2000} resulted in a reduced from 17% to 10%.

Before treatment, the O 1s peak (figure 2(c)), had a primary peak centred at 530.8 eV which is attributed to metal oxide and three smaller peaks which we attribute to surface oxygen species: OH^- , H_2O and C-O groups centred at 532.2 eV, 533.2 eV, 534.1 eV (labelled at S1, S2 and S3 in figure 2(c) [9, 17–21]). For all sample areas, after argon bombardment, the C-O component was reduced to the background and the H_2O component was not significantly altered, as indicated in the inset of figure 2(c)). Table 1 shows that argon bombardment with the cluster modes did not significantly alter the percentage OH^- of the total O 1s, however, the mono beam resulted in the reduction of OH^- groups on the surface of the ZnO nanorods. It can also be seen from the inset in figure 2(c) that there is a shift in the position of the O 1s from 530.8 eV to 530.5 eV (figure

S2 in the supplemental information shows a enlarge version of this inset with dashed lines to indicate the Fermi shift).

It has been suggested that reduction in the OH^- ions will result in a shift of the valance band and Fermi level to lower energy, resulting in upwards band bending and a shift from n-type to intrinsic ZnO [8–10]. Here the valance band has been scanned from 0 eV to 10 eV and the band edge fitted with a step-down function and the x -axis intercept was found by applying two tangents, as shown in figure S3(b) (see supplementary material). It can be seen from the scans in figure S3 and table 1 that argon bombardment with the clusters source did not significantly alter the position of the valance band edge, at 3.3 ± 0.1 eV. From table 1, it is clear that the treatment with 0.5 KeV $\text{Ar}^+_{\text{Mono}}$ caused a visible shift of 0.2 eV in the valance band edge, towards lower binding energy. The higher-powered treatment of 5 KeV $\text{Ar}^+_{\text{Mono}}$ results in a bigger shift towards lower binding energies of 0.3 eV, as shown in figure 2(d)). It was also observed that there was a Fermi shift of the oxygen peak to lower binding energies. This indicates there is upwards band bending for the ZnO nanowires from n-type towards intrinsic.

In our previous work we observed upwards band bending after the ZnO nanorods had been treated with argon bombardment resulting in a shift from Ohmic to Schottky contacts [11, 12]. We also observed with PL that the height of the DLE peak relative to the near band edge (NBE) also decrease with argon bombardment. Therefore, PL was also carried out on

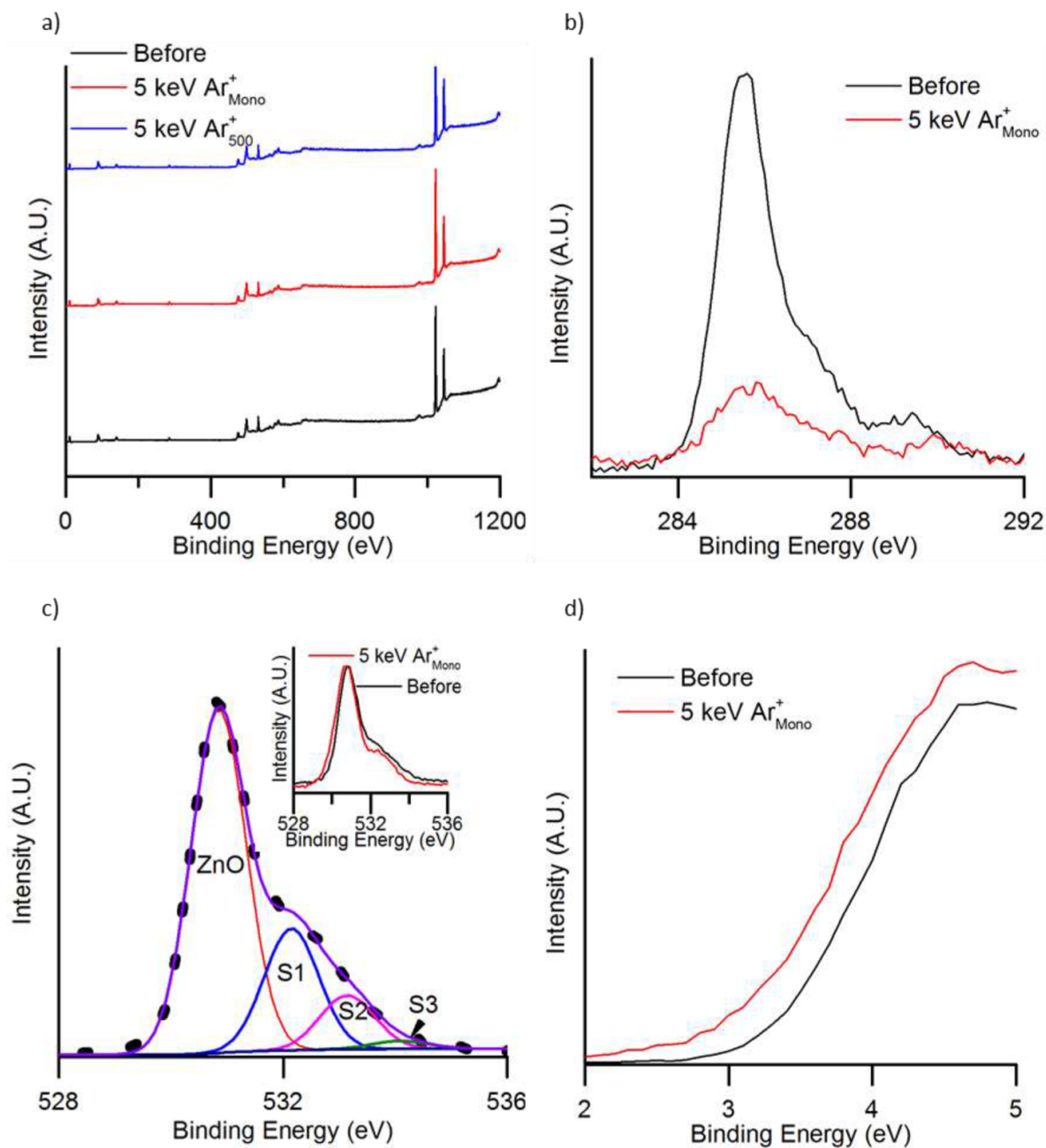


Figure 2. XPS scans of ZnO nanowires. (a) wide survey scans before and after 5 keV Ar⁺_{Mono} (offset by 1) and 5 keV Ar⁺₅₀₀ (offset by 2) (b) carbon 1s peak scans before and after 5 keV Ar⁺_{Mono}, (c) oxygen 1s with fitted components, envelope and background before treatment with the inset showing the raw data before and after 5 keV Ar⁺_{Mono} and (d) valence band edge before and after 5 keV Ar⁺_{Mono}.

Table 1. Atomic percentage carbon, OH⁻ as a percentage of total oxygen and valence band (VB) edge position before and after each treatment of argon bombardment.

Treatment	C before %	C after %	OH ⁻ before (% total O)	OH ⁻ after (% total O)	VB before (eV)	VB after (eV)
As grown	17 ± 1	–	23 ± 1	–	3.3 ± 0.1	
5 keV Ar ⁺ ₂₀₀₀	17 ± 1	10 ± 1	24 ± 1	22 ± 1	3.3 ± 0.1	3.3 ± 0.1
5 keV Ar ⁺ ₅₀₀	29 ± 1	20 ± 1	22 ± 1	22 ± 1	3.2 ± 0.1	3.3 ± 0.1
10 keV Ar ⁺ ₅₀₀	22 ± 1	11 ± 1	23 ± 1	22 ± 1	3.3 ± 0.1	3.3 ± 0.1
20 keV Ar ⁺ ₅₀₀	16 ± 1	4 ± 1	23 ± 1	24 ± 1	3.4 ± 0.1	3.4 ± 0.1
0.5 KeV Ar ⁺ _{Mono}	19 ± 1	10 ± 1	22 ± 1	19 ± 1	3.3 ± 0.1	3.1 ± 0.1
5 KeV Ar ⁺ _{Mono}	17 ± 1	4 ± 1	20 ± 1	15 ± 1	3.3 ± 0.1	3.0 ± 0.1

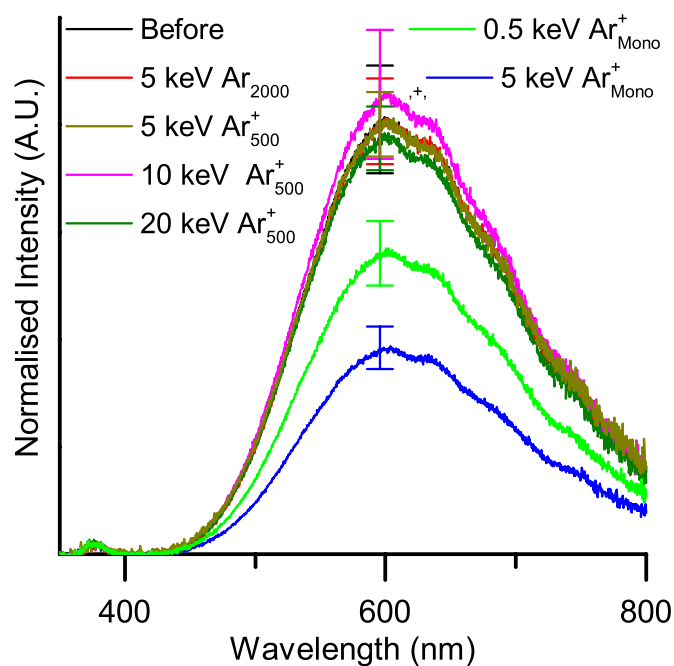


Figure 3. Normalised PL spectra of ZnO nanowires before and after argon bombardment. Error bars show standard deviation calculated at 595 nm.

each area that has been treated and the control area. In each area three spectra were taken, then normalised to the NBE peak and averaged. The PL spectra are shown in figure 3.

The NBE peak before argon bombardment was centred at 378 nm and the DLE peak has a main component centred at 595 nm as well as other components centred at 640 nm, 690 nm, and 765 nm. It should be noted that the relative difference in normalised intensity between the NBE peak and DLE on the samples measures here is considerably larger than that observed in our previous work [12, 22]. As the growth method is the same apart from the use of a spin coated zinc acetate seed layer annealed to convert to ZnO here compared to a ZnO PVD seed layer in our previous work, we suggest that the seed layer can have a significant effect on the observed defects.

Argon bombardment with the cluster modes did not significantly alter the relative intensity or shape of the DLE peak. It should be noted DLE peak of the 10 keV Ar^+_{500} sample is slightly higher than the other peaks, however, this is with the range of variance across the sample and is in line with the uncertainty in our previous work and is therefore not considered significant [11]. However, it can be seen from figure 3 that treatment with the monoatomic source causes the DLE peak to reduce relative to the NBE peak, with the more aggressive etch of 5 keV resulting in a reduction in the DLE peak to NBE peak ratio from 40:1 to 18:1. A similar result has been reported by Chen *et al* who used argon ion milling to bend ZnO nanowires and attribute their observation to the passivation of surface trapping sites during low energy Ar^+ milling [23].

There had been much debate in published literature over the origins of the DLE peak components and their links to defects, including the role of zinc and oxygen vacancies, interstitials, hydrogen impurities and density of states confinement

effects [24–31]. Trends in the literature suggest components situated at ~ 595 nm and ~ 640 nm are caused by charged oxygen vacancies which are considered to be donor defects [24–27, 32–34]. The components centred at ~ 690 nm and ~ 765 nm have been attributed to oxygen anti-sites and neutral oxygen vacancies, both considered acceptor states [27, 31–34].

4. Conclusion

ZnO nanorods have been synthesised hydrothermally and characterised using SEM, PL and XPS before and after argon bombardment. In our previous work [11, 12] we suggested that argon bombardment removed the surface contamination which results in improved consistency for the nano-scale contacts and reduced the overall measured resistance. Our results here confirm our assumption and show that argon bombardment reduces adventitious carbon.

Our work here also shows that high energy bombardment results in a decrease in defects measured with PL and damages the nanorod surface as well as causing an observed shift in the VB edge from 3.3 eV and 3 eV. This indicates upward band bending and a shift from n-type to a more intrinsic nature. This suggests that contact type and the electronic nature of ZnO can be manipulated using argon bombardment. Furthermore, using Ar surface stripping to first shift n-type ZnO to intrinsic may allow other processes to convert it to stable p-type ZnO which has so far been challenging [35]. This will allow advancements in device applications and devices such as light emitting diodes which require p-type ZnO [36].

Acknowledgments

Financial support was provided by the Flexible Integrated Energy Systems (FLEXIS) operations funded by the Welsh European Funding Office (WEFO) through the Welsh Government, the Office of Naval Research (N00014-15-2717), and the Robert A. Welch Foundation (C-0002). The Welsh Government is also acknowledged for Sêr Cymru II Fellowships (C E G and A O W) part funded by the European Regional Development Fund (ERDF).

ORCID iD

Chris J Barnett  <https://orcid.org/0000-0002-0139-836X>

References

- [1] Cheng H, Cheng J, Zhang Y and Wang Q 2007 Large-scale fabrication of ZnO micro- and nano-structures by microwave thermal evaporation deposition *J. Cryst. Growth* **299** 34–40
- [2] Schmidt-mende L and Macmanus-driscoll J L 2007 ZnO – nanostructures, defects, and devices *Mater. Today* **10** 40–48
- [3] Ra H, Choi K S, Ok C W, Jo S Y, Bai K H and Im Y H 2008 Ion bombardment effects on ZnO nanowires during plasma treatment Ion bombardment effects on ZnO nanowires during plasma treatment *Appl. Phys. Lett.* **93** 033112
- [4] Law J B K and Thong J T L 2008 Improving the NH₃ gas sensitivity of ZnO nanowire sensors by reducing the carrier concentration *Nanotechnology* **19** 205502

- [5] Liu K W, Chen R, Xing G Z, Wu T and Sun H D 2010 Photoluminescence characteristics of high quality ZnO nanowires and its enhancement by polymer covering *Appl. Phys. Lett.* **96** 023111
- [6] Richters J, Voss T, Kim D S, Scholz R and Zacharias M 2008 Enhanced surface-excitonic emission in ZnO/Al₂O₃ core – shell nanowires *Nanotechnology* **19** 305202
- [7] Dastjerdi H T, Prochowicz D and Yadav P 2020 Tuning areal density and surface passivation of ZnO nanowire array enable efficient PbS QDs solar cells with enhanced current density *Adv. Mater. Interfaces* **7** 1901551
- [8] Hyland A M, Makin R A, Durbin S M and Allen M W 2017 Giant improvement in the rectifying performance of oxidized Schottky contacts to ZnO *J. Phys. D: Appl. Phys.* **121** 024501
- [9] Heinhold R, Cooil S P, Evans D A and Allen M W 2014 Stability of the surface electron accumulation layers on the nonpolar (101 $\bar{0}$) and (112 $\bar{0}$) faces of ZnO *J. Phys. Chem. C* **118** 24575–82
- [10] McNeill A R, Bell K J, Hyndman A R, Gazoni R M, Reeves R J, Downard A J and Allen M W 2018 Synchrotron x-ray photoelectron spectroscopy study of electronic changes at the ZnO surface following aryldiazonium ion grafting : a metal-to-insulator transition *J. Phys. Chem. C* **122** 12681–93
- [11] Barnett C J *et al* 2018 Investigation into the effects of surface stripping ZnO nanosheets *Nanotechnology* **29** 165701
- [12] Barnett C J, Kryvchenkova O, Smith N A, Kelleher L, Maffei T G G and Cobley R J 2015 The effects of surface stripping ZnO nanorods with argon bombardment *Nanotechnology* **26** 415701
- [13] Kennedy O W *et al* 2019 Mapping the origins of luminescence in ZnO nanowires by STEM-CL *J. Phys. Chem. Lett.* **10** 386–92
- [14] Barnett C J *et al* 2012 Investigation into the initial growth parameters of hydrothermally grown zinc oxide nanowires *2012 12th IEEE Int. Conf. Nanotechnol* pp 1–4
- [15] Kitani H, Toyoda N, Matsuo J and Yamada I 1997 Incident angle dependence of the sputtering effect of Ar-cluster-ion bombardment *Nucl. Instrum. Methods Phys. Res. B* **121** 489–92
- [16] Comfort J H, Garverick L M and Reif R 1987 Silicon surface cleaning by low dose argon-ion bombardment for low-temperature (750 ° C) epitaxial silicon deposition *J. Phys. D: Appl. Phys.* **62** 3388
- [17] Byrne D, McGlynn E, Henry M O, Kumar K and Hughes G 2010 A novel, substrate independent three-step process for the growth of uniform ZnO nanorod arrays *Thin Solid Films* **518** 4489–92
- [18] Lupan O, Pauporté T, Tiginyanu I M, Ursaki V V, Şontea V, Ono L K, Cuenya B R and Chow L 2011 Comparative study of hydrothermal treatment and thermal annealing effects on the properties of electrodeposited micro-columnar ZnO thin films *Thin Solid Films* **519** 7738–49
- [19] Bang S, Lee S, Park J, Park S, Jeong W and Jeon H 2009 Investigation of the effects of interface carrier concentration on ZnO thin film transistors fabricated by atomic layer deposition *J. Phys. D: Appl. Phys.* **42** 235102
- [20] Lupan O, Chow L, Chai G, Roldan B, Naitabdi A, Schulte A and Heinrich H 2007 Nanofabrication and characterization of ZnO nanorod arrays and branched microrods by aqueous solution route and rapid thermal processing *Mater. Sci. Eng. B* **145** 57–66
- [21] Maffei T G G, Penny M W, Castaing A, Guy O J and Wilks S P 2012 Surface Science XPS investigation of vacuum annealed vertically aligned ultralong ZnO nanowires *Surf. Sci.* **606** 99–103
- [22] Barnett C J, Mourgelas V, McGettrick J D, Maffei T G G, Barron A R and Cobley R J 2019 The effects of vacuum annealing on the conduction characteristics of ZnO nanorods *Mater. Lett.* **243** 144–7
- [23] Chen R, Ye Q-L, He T C, Wu T and Sun H D 2011 Uniaxial tensile strain and exciton – phonon coupling in bent ZnO nanowires *Appl. Phys. Lett.* **98** 241916
- [24] Liao Z, Zhang H-Z, Zhou Y-B, Xu J, Zhang J-M and Yu D-P 2008 Surface effects on photoluminescence of single ZnO nanowires *Phys. Lett. A* **372** 4505–9
- [25] Janotti A and Van De Walle C G 2007 Native point defects in ZnO *Phys. Rev. B* **76** 1–22
- [26] Janotti A, Van De Walle C G and Janotti A 2005 Oxygen vacancies in ZnO *Appl. Phys. Lett.* **87** 122102
- [27] Li L 2017 On the double-band luminescence of ZnO nanoparticles On the double-band luminescence of ZnO nanoparticles *EPL* **117** 67005
- [28] Wei X Q, Man B Y, Liu M, Xue C S, Zhuang H Z and Yang C 2007 Blue luminescent centers and microstructural evaluation by XPS and Raman in ZnO thin films annealed in vacuum, N₂ and O₂ *Physica B* **388** 145–52
- [29] McCluskey M D and Jokela S J 2009 Defects in ZnO *J. Phys. D: Appl. Phys.* **106** 071101
- [30] Yousefi R and Kamaluddin B 2009 Applied Surface Science Fabrication and characterization of ZnO and ZnMgO nanostructures grown using a ZnO/ZnMgO compound as the source material *Appl. Surf. Sci.* **256** 329–34
- [31] Liu J, Lee S, Ahn Y H, Park J and Koh K H 2009 Tailoring the visible photoluminescence of mass-produced ZnO nanowires *J. Phys. D: Appl. Phys.* **42** 095401
- [32] Xu P S, Sun Y M, Shi C S, Xu F Q and Pan H B 2003 The electronic structure and spectral properties of ZnO and its defects *Nucl. Instrum. Methods Phys. Res. B* **199** 286–90
- [33] Oba F, Choi M, Togo A and Tanaka I 2011 Point defects in ZnO: an approach from first principles *Sci. Technol. Adv. Mater.* **12** 034302
- [34] Heo Y W, Norton D P and Pearton S J 2005 Origin of green luminescence in ZnO thin film grown by molecular-beam epitaxy by molecular-beam epitaxy *J. Phys. D: Appl. Phys.* **98** 073502
- [35] Lu M, Lu M and Chen L 2012 p-Type ZnO nanowires : from synthesis to nanoenergy *Nano Energy* **1** 247–58
- [36] Ryu Y R, Zhu S, Look D C, Wrobel J M, Jeong H M and White H W 2000 Synthesis of p-type ZnO *J. Cryst. Growth* **216** 330–4